Quantitative Approach to Studying Film Pollution of the Sea Surface Using Satellite Imagery

V. V. Zamshin ✉, E. R. Matrosova, V. N. Khodaeva, O. I. Chvertkova

AEROCOSMOS Research Institute for Aerospace Monitoring, Moscow, Russian Federation
✉ *viktor.v.zamshin@gmail.com*

Purpose. Numerous studies of various film pollutions (oil spills, surfactants etc.) are performed by means of satellite monitoring of seas and oceans. However, the problem of formal ranking the water areas of the regions under study by frequency and intensity of pollution is still unsolved. The conditions and periodicity of satellite survey can differ greatly depending on the monitoring region that determines both spatial variability of the probability of film pollution detection and the need to take this feature into consideration. Here we attempt to develop a quantitative approach to studying the sea surface film pollutions based on processing of large volumes of satellite optical and radar imagery.
Methods and Results. The concept "index of sea surface exposure to film pollutions", d_{fpMON}, and the method for calculating its quantitative value on a regular spatial grid are proposed. The value of d_{fpMON} is defined as a ratio of the pollution area observed at the site to the area of the analyzed resolution elements (where detection of film pollution is theoretically possible). Within the framework of this approach, the already existing methods for analyzing the results of long-term satellite seawater pollution monitoring were improved due to taking into account the meteorological conditions and the spatial distribution of the observation amount. Having been applied, the proposed approach permitted to study spatial distribution of the non-biogenic film pollutions in the northern part of the Black Sea; they were detected resulting from interpretation of 4428 satellite images obtained in 2019 by the *Landsat*-8, *Sentine*l-2*A/B* and Sentinel-1*A/B* satellites (2499 cases of pollution processed). The average value of the d_{fpMON} index was 0.012%. Three regions, where the d_{fpMON} values exceeded the average one by more than 30 times were identified.
Conclusions. The example of a site in the northern Black Sea has shown the possibility of obtaining representative information products of **satellite oceanography**, which quantitatively characterize spatial variability of the sea surface **film** pollution recorded during the long-term episodes of satellite monitoring.

Keywords: Earth remote sensing, sea surface, film pollutions, oil slicks, optical survey, multispectral imagery, radar imagery, satellite oceanography, Black Sea

1. INTRODUCTION

A large amount of film pollution (FP) studies in the seas and oceans, the examples of which are [1–6], were carried out using the satellite survey. The analysis of contemporary level of studies, carried out within this theme, allows us to point out certain unsolved problems.

The most well-known problem is associated with the difficulty of interpreting the sea surface FP. This applies to both multispectral and radar satellite images. There are various FP classifications, according to which pollution can be subdivided,

for example, into mineral and biogenic, natural and anthropogenic. The problem of identifying the films of various types in the sea surface satellite images has been discussed in numerous works, for instance, in [1, 2, 5, 7, 8]. Despite the difficulties, visual interpretation of satellite images, performed by trained specialists, in combination with the capabilities of the so-called geoinformational approach [9], allows to obtain generally adequate results.

Another problem is related to obtaining the quantitative estimates of the results of FP detection. Usually [2], the study is reduced to the formation of generalized map-schemes of the detected and type-classified FP, as well as to the comparison of these diagrammatic maps with a situational map using geoinformation technologies [9–12]. This approach provides a significant advance in the analysis of the features and causes of the detected FPs. However, at the same time, the problem of formal classification of the areas of the studied water site according to the pollution frequency and intensity remains unsolved. It is especially difficult to carry out a quantitative comparison of the monitoring results obtained for different seas, since the conditions and frequency of satellite surveys can vary significantly.

In [4, 10, 13, 14], the authors advanced deeper in the development of approaches to the quantitative analysis of data on the detected FP of the sea areas: the estimates obtained during the monitoring correlate with the number of observations or hours of observations (for aviation research methods). In [14], the approach to the FP analysis is the most perfect: the authors carry out a spatial-temporal analysis of the regions distribution of the recorded FP, correlated with the map of the number of satellite surveys, which makes it possible to obtain more relevant assessments of water areas susceptibility to pollution. However, the work still does not take into account the meteorological factor (with a formally performed survey, the possibility of observing the FP of the sea surface may be absent due to unfavorable meteorological conditions, which actually reduces the number of observations).

In this study, an attempt of further development of a quantitative approach to the FP study of the sea surface vast areas according to the satellite survey data was made. The workflow of processing and analysis of interpreting (FP detecting) the results of large volumes of satellite multispectral and radar images of the sea surface, taking into account variations in meteorological conditions and the spatial distribution of the frequency of performing relevant surveys by various satellite systems (SS), is considered.

2. METHOD

We consider the case of a one-time observation from space of the underlying surface certain section and express the registration results of given-type FP type as its area percentage (%):

$$d_{\mathrm{fp}} = \frac{s_{\mathrm{fp}}}{s_{\mathrm{i}}} \cdot 100\%, \tag{1}$$

where d_{fp} is a proportion of the section water area under observation characterized by FP; s_{fp} is an area marked as "FP" by the interpreters; s_{i} is a water surface area subjected to interpretation.

In this case, the value

$$d_{\text{fpCC}} = \frac{\sum_i (s_{\text{fpSS}})_i}{\sum_i (s_{\text{iSS}})_i} \cdot 100\% \tag{2}$$

will demonstrate averaged over the entire monitoring period share of FP area of the selected area of the water surface, observed using a specific SS (i denotes the serial number of the survey).

At different i, the value s_{fpSS} takes different values:

$$(s_{\text{fpSS}})_i = (n_{\text{fpSS}})_i \cdot s_{\text{pixSS}}, \tag{3}$$

where n_{fpSS} is an amount of pixels corresponding to FP; s_{pixSS} is a pixel area for the selected SS.

We note that s_{pixSS} value (the water surface area subjected to interpretation) for the same area for different i also takes different values, since the analyzed area, depending on the shooting episode, can:

a) not be completely covered by survey;

b) be characterized by unfavorable meteorological conditions, which do not allow observing FP even in the presence of survey results.

We will separately focus on the peculiarities of accounting for hydrometeorological conditions using the example of the three most efficient satellite radar and multispectral systems *Sentinel*-1*A/B*, *Sentinel*-2*A/B*, *Landsat*-8, which are used to interpret the FP of various types (Table 1). The values of n_{hm} (the number of the water surface observed pixels for which the hydrometeorological conditions were within acceptable limits) for each site and episode of the survey can be obtained based on the processing of additional data. As is known [2–4, 8, 11, 12, 14], for the FP detection by satellite radar systems, an important hydro-meteorological factor is the wind speed, which, according to some studies, should be within the range from 2 to 9 m/s [15]. In order to use satellite multispectral data, the absence of dense clouds is required.

As can be seen from Table 1, *NCEP Climate Forecast System Version 2* data supplied as spatial distributions at six-hour intervals were used to determine wind conditions corresponding to the time and location of the radar survey. For taking into account the conditions for multispectral imaging, we used cloud cover masks included into the standard *USGS Landsat 8 Collection* 1 *Tier* 1 *TOA Reflectance* and *Sentinel*-2 *MSI: MultiSpectral Instrument, Level*-2A products.

Based on the foregoing,

$$(s_{\text{iSS}})_i = (n_{\text{hmSS}})_i \cdot s_{\text{pixSS}}, \tag{4}$$

where n_{hmSS} is a number of observed water area pixels for which hytrometeorological conditions were within acceptable limits.

The fundamental importance of taking into account the number of performed relevant (with regard to hydrometeorological conditions) observations can be demonstrated by an example. In Fig. 1 the maps formed according to formula (4) for the Black Sea northern part, obtained for the date interval from 01.01.2019 to 31.12.2019 inclusive, are given. The total number of recorded images was 4428. 211 of them were obtained from *Landsat*-8 satellite, 2864 – by *Sentinel*-2*A/B* satellite system, and 1353 – by *Sentinel*-1*A/B* satellite system.

Methods applied for quantifying the pixels in the processed fragments of satellite images (n_{hmSS})$_i$, at which detection of the film pollution is considered theoretically possible

Step of processing	Radar SS	Multispectral SS	
	Sentinel-1	*Landsat*-8	*Sentinel*-2
Step 1	Formation of an image fragment corresponding to the analyzed area		
Step 2	Excluding (masking) of the pixels which are outside the monitoring area, and those corresponding to land, from the fragment		
Step 3	Selection of the near-surface wind speed data based on date and time of the survey from the archive *NCEP Climate Forecast System Version* 2	Exclusion of the pixels for which the condition is met (presence of a cloud marker in the quality assessment band *BQA*)	Exclusion of pixels for which the condition is met (presence of a cloud marker in the scene classification band *SCL*)
Step 4	Exclusion of the pixels falling on the areas where the wind speed $V < 2$ m/s or $V > 9$ m/s		
Step 5	Calculation of a number of remaining pixels (not masked in steps 1–4)		
Result	(n_{hmS1})$_i$	(n_{hmL8})$_i$	(n_{hmS2})$_i$

Fig. 1 demonstrates that *Landsat*-8 multispectral satellite system made it possible to perform the smallest number of observations (within the area, the values vary mainly in the range from ~ 10 to ~ 60 observations). In the second place in terms of productivity was *Sentinel*-2*A*/*B* multispectral satellite system (within the area, the values vary approximately in the range from ~ 70 to ~ 150 observations). Most often, the survey was carried out from *Sentinel*-1*A*/*B* radar satellites (from ~ 110 to ~ 240 observations in 2019, depending on the specific section of the research area). The total number of observations per year for all three SS reached 467 at some points of the site. Taking into account the meteorological conditions, the number of relevant observations, which were used for interpretation, varied within the site mainly in the range from 150 to 300 observations per year (Fig. 1, *e*). The strong spatial variability of the number of performed observations indicates the

need to take this factor into account when assessing the results of interpreting the FP, which is implemented in the proposed approach.
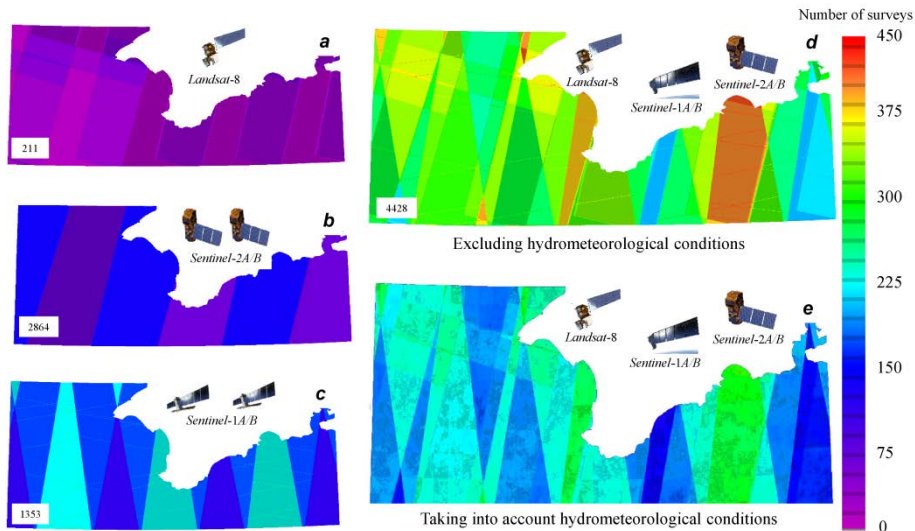

F i g. 1. Maps of spatial distributions of a number of observations in 2019 for the northern part of the Black Sea carried out in from the *Landsat*-8 (*a*), *Sentinel*-2*A*/*B* (*b*) and *Sentinel*-1*A*/*B* (*c*) satellites, and maps of distribution of a number of total observations with no account (*d*) and with account (*e*) for cloudiness and unfavorable wind conditions

Summarizing the monitoring results obtained from several SS, taking into account formulas (2) – (4), for any selected section of the studied water area, it is possible to calculate the relation

$$d_{\text{fpMON}} = \frac{\sum_{j=1}^{Y}\left(s_{\text{pixSS}j}\cdot\sum_{1}^{X}(n_{\text{fpSS}j})_i\right)}{\sum_{j=1}^{Y}\left(s_{\text{pixSS}j}\cdot\sum_{1}^{X}(n_{\text{hmSS}j})_i\right)} \cdot 100\%, \tag{5}$$

where Y is a number of applied remote probing SS; j is a counting number of SS ($j = 1, …, Y$); $S_{\text{pixSS}j}$ is a pixel area for j^{th} SS; X is a number of surveys for the selected SS; i is a counting number of survey ($I = 1, ..., X$); $(n_{\text{fpSS}j})_i$ is an amount of pixels corresponding to FP registered as a result of interpreting the results of ith survey; $(n_{\text{hmSS}j})_i$ is a number of observed water areas pixels for which the hydrometeorological conditions during the ith survey were within the acceptable limits.

The numerator of formula (5) shows the total amount of FP observed at the site using all applied SS, expressed in area units. The denominator of formula (5) shows the total amount (expressed in units of area) of those resolution elements of all analyzed images on which it was theoretically possible to detect FP.

The essence of the proposed approach is to obtain the spatial distribution of the value of d_{fpMON}, calculated by formula (5). Within the framework of this study, this value is called the «index of the sea surface "exposure to FP" (%).

Next, an example of application of the proposed approach for monitoring the FP in the northern part of the Black Sea will be considered.

3. RESULTS AND DISCUSSION

Now we are to consider an example of the implementation of the proposed approach for monitoring a non-biogenic origin FP (natural oil and gas manifestations, ship and coastal discharges, spills at offshore oil and gas platforms, leaks of subsea pipelines) in the Black Sea northern part in the period from 01.01.2019 to 31.12.2019. This area was well studied earlier [4, 11, 14, 16, 17], which makes it possible to assess the adequacy of the results obtained in our study. The choice of the site was also determined by a significant number of non-biogenic origin FP sources (shipping routes, oil and gas seeps) located within its boundaries [12, 18–20].

In this work, an array of 4428 pre-interpreted satellite images obtained from *Landsat*-8, *Sentinel*-1*A/B*, *Sentinel*-2*A/B* satellites from 01.01.2019 to 31.12.2019 was used as the initial data. The spatial distributions of the number of performed relevant observations $(n_{\mathrm{hmSS}j})_i$ for these SS in the study area were demonstrated above (Fig. 1). The total area of the used sea surface satellite images was ~ 25.7 million km², while the interpreted area $(s_{\mathrm{iSS}})_i$, corresponding to permissible meteorological conditions, was ~ 18.2 million km². Thus, unfavorable weather conditions accompanied ~ 29% of the original satellite data. For *Landsat*-8 data, the interpreted area (s_{iL8}) was ~ 1.6 million km², for *Sentinel*-2*A/B* (s_{iS2}) ~ 5.5 million km², for *Sentinel*-1*A/B* (s_{iS1}) ~ 11.1 million km². The relation of satellite images interpreted area to the investigated water surface area was ~ 229 (as many times, on average, each of the fragments of the water area was monitored).

During the interpretation, a team of interpretation operators identified 2,499 non-biogenic film formations of anthropogenic and natural origin, including ship spills, waste water discharges, spills at offshore oil and gas platforms, as well as films formed on the sea surface as a result of activation of underwater sources of hydrocarbons (mud volcanoes, vultures, griffins and others) (Fig. 2).
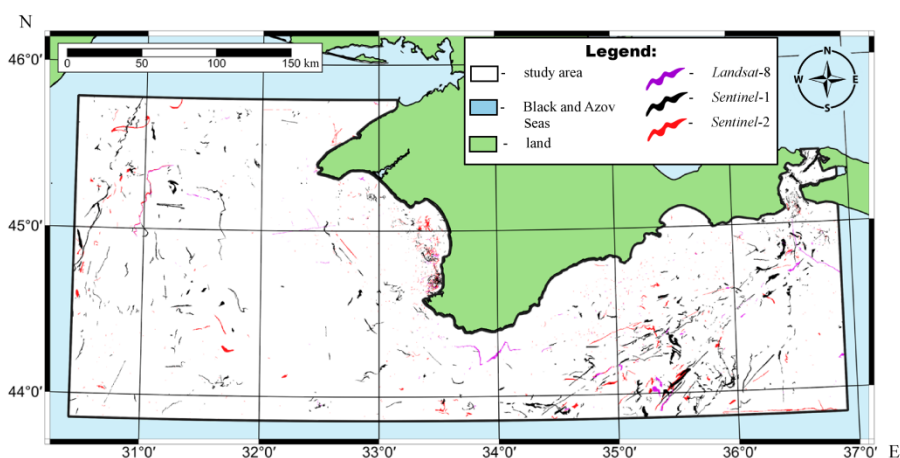

F i g. 2. Map of non-biogenic film pollutions revealed from 01.01.2019 to 31.12.2019 as a result of interpreting the data from the satellites *Landsat*-8 (purple polygons), *Sentinel*-2*A/B* (red polygons) and *Sentinel*-1*A/B* (black polygons) at the test site

Analysis of Fig. 2 shows that the areas of concentration of the studied type FP, detected by different SS, on the whole coincide, i.e. one can indicate the mutual support of the processing results of satellite multispectral and radar images obtained using different SS. The total area of the discovered non-biogenic FP was ~ 2.1 thousand km^2.

We will divide the monitoring area into N square fragments and will calculate $(d_{fpMON})_f$ (see formula (5)) for each of them ($f = 1, 2, …, N$). The n_{fpSS} values are calculated on the basis of processing the results of the decryption of objects of interest performed interpretation, presented in the raster masks form, by summing the values of all pixels included into the processed fragment (the pixels corresponding to the object of interest have a value of 1, background – 0). The map of spatial distribution index of water surface exposure to non-biogenic FP, obtained using the proposed quantitative approach for the Black Sea test area, is shown in Fig. 3.
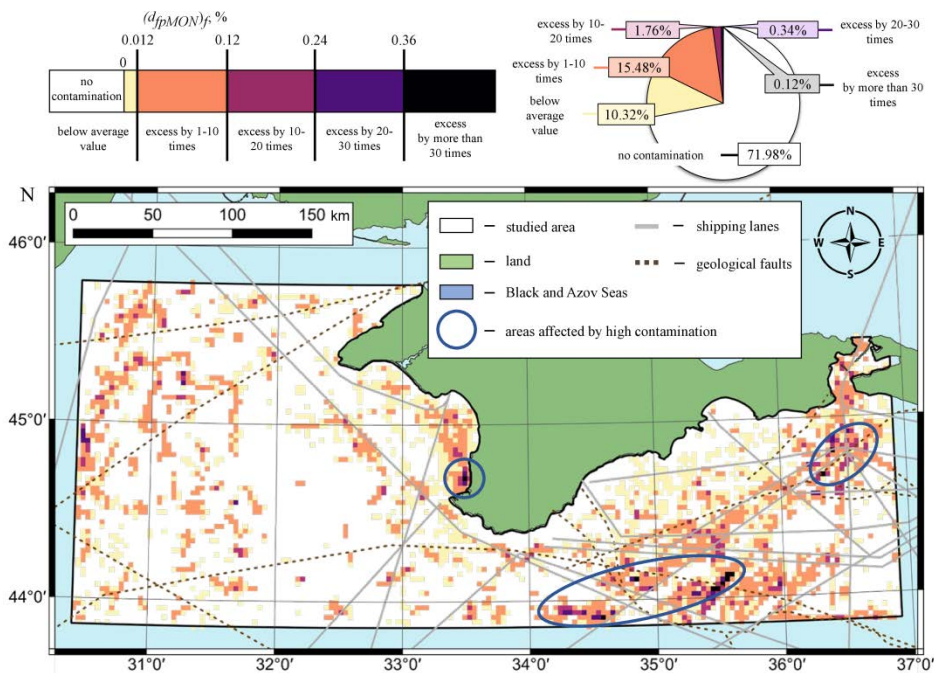

F i g. 3. Spatial distribution of the values of the index of sea surface exposure to film pollutions, $(d_{fpMON})_f$, of non-biogenic origin calculated for each cell (3 × 3 km^2) of the water area under study based on the results of interpreting the data from the *Landsat*-8, *Sentinel*-2A/B and *Sentinel*-1A/B satellites obtained in 2019

The map is presented in 3 km resolution (the number of analyzed water area fragments was N = 8857). Information products of this type can be obtained for any arbitrary cell size.

Analysis of the map shown in Fig. 3, demonstrates that within the study region on ~ 72% of the area, non-biogenic FP were never observed in 2019. Areas characterized by an indicator of susceptibility to pollution with a value below the average for the water area make up ~ 10% of the study region area. The remaining areas (~ 18% of the site area) are characterized by an index of exposure to pollution equal to or higher than the average value (Fig. 2). In general, high rates of susceptibility to non-biogenic FP are observed along shipping routes and geological faults, which is consistent with the results of previous studies [4, 12, 14]. At the same time, based on the results of this study, three zones in which the cells are concentrated with an excess of the average indicator of exposure to pollution of this type by more than 30 times, can be identified: near Sevastopol, near the Kerch Strait, the southeastern part of the test site (blue ellipses on Fig. 3).

The generalized quantitative characteristics obtained as a result of the propo-sed approach application to the study of non-biogenic origin FP in the test area of the Black Sea in 2019 are given in Table. 2.

T a b l e 2

Generalized quantitative characteristics of the non-biogenic film pollution monitoring performed using the proposed approach in the northern Black Sea in 2019

Characteristic	Satellite system			Total
	Landsat-8	*Sentinel*-2	*Sentinel*-1	
Number of surveys N, unit	211	2864	1353	4428
Interpreted area S_i, million km^2	1.6	5.5	11.1	18.2
Number of objects N_{fp}, unit	209	952	1338	2499
Area of objects S_{fp}, km^2	170	514	1441	2126
Portion of the pollution area relative to the interpreted area d_{fpMON}, %	0.010	0.009	0.013	0.012

N o t e. The objects of interpretation for all the satellite systems are the visually interpreted film pollutions of non-biogenic origin (ship spills, natural hydrocarbon discharges, waste water discharges etc.).

As can be seen from Table 2, the share of the surface area covered by the FP of the investigated type relative to the total interpreted satellite images area is 0.012%. This means that within the study area it is possible to meet a non-biogenic FP at an arbitrary point on the sea surface at an arbitrary time moment with a probability of

~ 0.012% (in 12 out of 100 thousand cases). The relatively low value of this indicator is due to the fact that the density of pollution is significant only in certain zones of the water area (Fig. 3). When calculating this indicator separately for each SS, the following results were obtained: for *Landsat*-8 – 0.010%, for *Sentinel*-2 – 0.009%, for *Sentinel*-1 – 0.013%. These values are generally close to each other, which indicates the adequacy of such estimates and their consistency even in the case of using only one of the three involved Earth remote sensing systems. The maximum value of the fraction of the water surface covered by FP was obtained on the basis of processing satellite radar images (*Sentinel*-1), which may be a consequence of both the high sensitivity of the radar data to FP, and the involvement of a certain number of falsely recognized objects in the analysis due to formation specificity of the sea surface satellite radar images [1, 3, 5, 21].

4. CONCLUSION

An approach to the study of the sea surface film pollution, which involves the calculation of quantitative value "index of the sea surface exposure to film pollution" on a regular spatial grid based on algorithmized processing of the results of interpreting time series of satellite multispectral and radar images, is considered. By means of taking into account variations in meteorological conditions and the spatial distribution of the number of observations, the proposed approach develops the known methods for analyzing the results of long-term satellite monitoring of marine film pollution.

On the example of a section of the Black Sea northern part, the possibility of obtaining representative information products of a new type, quantitatively characterizing the spatial variability of the sea surface pollution recorded during the long-term episodes of satellite monitoring, has been demonstrated. In the given example, non-biogenic film pollutions were used as objects of interest. However, the proposed approach can be used in the interests of studying other areal (non-point) formations on the sea surface. The classes of the objects under study are determined by the process of interpreting satellite images.

With the development of methods for automatic interpretation of large streams of sea surface satellite images, in the interests of detecting film formations of various types (see, for example, [21]), prospects for the practical application of the considered approach are opening up. In the near future, the possibility of forming regularly updated, quantitatively comparable standardized information products that characterize the spatial distribution of film formations in sea areas seems realistic.

REFERENCES

1.   Ivanov, A.Yu., 2007. Slicks and Oil Films Signatures on Syntetic Aperture Radar Images. *Issledovanie Zemli iz Kosmosa*, (3), pp. 73-96 (in Russian).

2.   Lavrova, O.Yu. and Mityagina, M.I., 2013. Satellite Monitoring of Oil Slicks on the Black Sea Surface. *Izvestiya, Atmospheric and Oceanic Physics*, 49(9), pp. 897-912. https://doi.org/10.1134/S0001433813090107

3. Fingas, M. and Brown, C., 2013. Oil Spill Remote Sensing. In: J. Orcutt, ed., 2013. *Earth System Monitoring*. New York: Springer, pp. 337-388. https://doi.org/10.1007/978-1-4614-5684-1_15

4. Ivanov, A.Yu., Kucheiko, A.A., Filimonova, N.A., Kucheiko, A.Yu., Evtushenko, N.V., Terleeva, N.V. and Uskova, A.A., 2017. Spatial and Temporal Distribution of Oil Spills in the Black Sea and the Caspian Sea Based on SAR Images: Comparative Analysis. *Issledovanie Zemli iz Kosmosa*, (2), pp. 13-25. https://doi.org/10.7868/S0205961417020038 (in Russian).

5. Skrunes, S., Johansson, A.M. and Brekke, C., 2019. Synthetic Aperture Radar Remote Sensing of Operational Platform Produced Water Releases. *Remote Sensing*, 11(23), 2882. https://doi.org/10.3390/rs11232882

6. Ivonin, D., Brekke, C., Skrunes, S., Ivanov, A. and Kozhelupova, N., 2020. Mineral Oil Slicks Identification Using Dual Co-polarized Radarsat-2 and TerraSAR-X SAR Imagery. *Remote Sensing*, 12(7), 1061. https://doi.org/10.3390/rs12071061

7. Bondur, V.G., 2011. Aerospace Methods and Technologies for Monitoring Oil and Gas Areas and Facilities. *Izvestiya, Atmospheric and Oceanic Physics*, 47(9), pp. 1007-1018. https://doi.org/10.1134/S0001433811090039

8. Mityagina, M.I., Lavrova, O.Yu. and Bocharova, T.Yu., 2015. Satellite Monitoring of Oil Pollution of the Sea Surface. *Sovremennye Problemy Distantsionnogo Zondirovaniya Zemli iz Kosmosa*, 12(5), pp. 130-149. Available at: http://d33.infospace.ru/d33_conf/sb2015t5/130%E2%80%93149.pdf [Accessed: 10 March 2021] (in Russian).

9. Ivanov, A.Yu. and Zatyagalova, V.V., 2008. A GIS Approach to Mapping Oil Spills in a Marine Environment. *International Journal of Remote Sensing*, 29(21), pp. 6297-6313. https://doi.org/10.1080/01431160802175587

10. Bulycheva, E.V., Kostianoy, A.G. and Krek, A.V., 2016. Interannual Variability of Sea Surface Oil Pollution in the Southeastern Baltic Sea in 2004−2015. *Sovremennye Problemy Distancionnogo Zondirovaniya Zemli iz Kosmosa*, 13(4), pp. 74-84. https://doi.org/10.21046/2070-7401-2016-13-4-74-84 (in Russian).

11. Ivanov, A. and Matrosova, E., 2019. Technogenically Provoked Seepage Activity in the Northwestern Part of the Black Sea According to Data from Space. *Ecology and Industry of Russia*, 23(8), pp. 57-63. https://doi.org/10.18412/1816-0395-2019-8-57-63 (in Russian).

12. Mityagina, M. and Lavrova, O., 2016. Satellite Survey of Inner Seas: Oil Pollution in the Black and Caspian Seas. *Remote Sensing*, 8(10), 875. https://doi.org/10.3390/rs8100875

13. Carpenter, A., 2019. Oil Pollution in the North Sea: the Impact of Governance Measures on Oil Pollution over Several Decades. *Hydrobiologia*, 845(1), pp. 109-127. https://doi.org/10.1007/s10750-018-3559-2

14. Ferraro, G., Meyer-Roux, S., Muellenhoff, O., Pavliha, M., Svetak, J., Tarchi, D. and Topouzelis, K., 2009. Long Term Monitoring of Oil Spills in European Seas. *International Journal of Remote Sensing*, 30(3), pp. 627-645. https://doi.org/10.1080/01431160802339464

15. Lavrova, O.Yu., Mityagina, M.I. and Kostianoy, A.G., 2016. *Satellite Methods for Detecting and Monitoring Marine Zones of Ecological Risk*. Moscow: SRI RAS, 334 p. Available at: http://www.iki.rssi.ru/books/2016lavrova.pdf [Accessed: 10 March 2021] (in Russian).

16. Bondur, V.G., Ivanov, V.A., Vorobiev, V.E., Dulov, V.A., Dolotov, V.V., Zamshin, V.V., Kondratiev, S.I., Lee, M.E. and Malinovsky, V.V., 2020. Ground-to-Space Monitoring of Anthropogenic Impacts on the Coastal Zone of the Crimean Peninsula. *Physical Oceanography*, 27(1), pp. 95-107. https://doi.org/10.22449/1573-160X-2020-1-95-107

17. Kruglyakova, R.P., Kruglyakova, M.V. and Shevtsova, N.T., 2009. Geological-Geochemical Characterization of Hydrocarbon Natural Shows in the Black Sea. *Geology and Mineral Resources of World Ocean*, (1), pp. 37-51. Available at: https://cyberleninka.ru/article/n/geologo-geohimicheskaya-harakteristika-estestvennyh-proyavleniy-uglevodorodov-v-chernom-more/viewer [Accessed: 15 March 2021] (in Russian).

18. Bondur, V.G., Zamshin, V.V., Zamshina, A.Sh. and Vorobyev, V.E., 2020. Registering from Space the Features of Deep Wastewater Outfalls into Coastal Water Areas Due to Discharge Collector Breaks. *Izvestiya, Atmospheric and Oceanic Physics*, 56(9), pp. 979-988. https://doi.org/10.1134/S0001433820090066

19. Glumov, I.F., Gulev, V.L., Senin, B.V. and Karnaukhov, S.M., 2014. *Regional Geology and Prospects of Oil and Gas Content in the Black Sea Deep-Water Basin and Adjacent Shelf Zones*: in two volumes. Part 1]. Moscow: Izdatel'skiy dom Nedra, 273 p. (in Russian).

20. Nemirovskaya, I.A., Onegina, V.D. and Konovalov, B.V., 2017. Hydrocarbons in the Suspended Matter and the Bottom Sediments in Different Regions of the Black Sea Russian Sector. *Physical Oceanography*, (4), pp. 46-58. https://doi.org/10.22449/1573-160X-2017-4-46-58

21. Krestenitis, M., Orfanidis, G., Ioannidis, K., Avgerinakis, K., Vrochidis, S. and Kompatsiaris, I., 2019. Oil Spill Identification from Satellite Images Using Deep Neural Networks. *Remote Sensing*, 11(15), 1762. https://doi.org/10.3390/rs11151762

About the authors:

Viktor V. Zamshin, Research Associate, AEROCOSMOS Research Institute for Aerospace Monitoring (4 Gorokhovsky Lane, Moscow, 105064, Russian Federation)**, ORCID ID: 0000-0003-4285-172X**, **ResearcherID: G-3224-2014**, **Scopus Author ID: 57205502046**, viktor.v.zamshin@gmail.com

Ekaterina R. Matrosova, Junior Research Associate, AEROCOSMOS Research Institute for Aerospace Monitoring (4 Gorokhovsky Lane, Moscow, 105064, Russian Federation)**, ORCID ID: 0000-0003-2719-6210**, **ResearcherID: AAG-1442-2021**, **Scopus Author ID: 57216743579**, ematrosova95@gmail.com

Vasilisa N. Khodaeva, Junior Research Associate, AEROCOSMOS Research Institute for Aerospace Monitoring (4 Gorokhovsky Lane, 105064, Moscow, Russian Federation)**, ORCID ID: 0000-0002-8913-5555**, **ResearcherID: AAG-1392-2021**, **Scopus Author ID: 57222296283**, vasilisak.95@gmail.com

Olga I. Chvertkova, Junior Research Associate, AEROCOSMOS Research Institute for Aerospace Monitoring (4 Gorokhovsky Lane, Moscow, 105064, Russian Federation), **ORCID ID: 0000-0002-6097-9762**, **ResearcherID: AAG-1420-2021**, **Scopus Author ID: 57221663635**, chvertkovaolga@gmail.com